Liu, D. *et al.* (2019). *Géotechnique* **69**, No. 9, 841–846 [https://doi.org/10.1680/jgeot.18.P.015]

TECHNICAL NOTE

Critical state of polymer-coated sands

DEYUN LIU*, SÉRGIO D. N. LOURENÇO† and JUN YANG‡

The water-repellent behaviour of polymers such as polydimethylsiloxane enables them to be utilised as coatings in soil particles to control wetting, with potential applications in barriers and fills. However, little information exists on the mechanics of coated soils. Here, the mechanical behaviour of a coated sand subjected to two mass ratios of dimethyldichlorosilane (0·05% and 3%) was investigated by triaxial tests. Dimethyldichlorosilane was mixed with the sand to produce polydimethylsiloxane coatings. Damage to the polymer coatings was investigated by interferometry. The results revealed that for a low mass ratio of dimethyldichlorosilane (0·05%), the shear strength and critical state locus are similar to those of natural sand; whereas for a high mass ratio of dimethyldichlorosilane (3%), there is a marked reduction of the shear strength, with the critical state locus showing a significant difference compared to that of natural sand. The quantification of roughness prior to and after the triaxial tests confirms the damage to the polymer coatings, with the effect of the coatings diminishing with the rise of stress level. The findings highlight the importance of the thickness of the coatings, with the 0·05% coated sand sufficient to manipulate the soil's hydraulic behaviour and the 3% coated sand opening new possibilities to manipulate the soil's mechanical behaviour.

KEYWORDS: laboratory tests; particle-scale behaviour; sands; shear strength

INTRODUCTION

Synthetic water-repellent granular materials exhibit a hydraulic and mechanical behaviour that is distinct from wettable granular materials (e.g. Bardet *et al.*, 2009; Byun *et al.*, 2011; Lee *et al.*, 2015). The wettability state of the coatings dictates whether the soil wets or not and the extent of wetting (Doerr *et al.*, 2000).

In geotechnical engineering, potential applications of synthetic water-repellent soils include their use in barriers or as fill materials (Zheng *et al.*, 2017), among others. Therefore, prediction of the mechanical behaviour of coated water-repellent soils is essential and is currently lacking in the literature. Lee *et al.* (2015) and Byun *et al.* (2011) found a decreased friction angle and shear strength for a water-repellent soil modified by an organo-silane (n-octyltriethoxysilane), while Bardet *et al.* (2011) illustrated unaffected friction angles for wax-coated sand. However, most related studies have been carried out in dry or unsaturated conditions with no control of suction, which could influence the mechanical behaviour and lead to conflicting results (Lechman *et al.*, 2006; Lourenço *et al.*, 2018).

The effect of stress level on soft, polymer coatings should be considered. The Young's modulus of polydimethylsiloxane (PDMS) ranges from 360 kPa to 870 kPa (Lötters *et al.*, 1997; Armani *et al.*, 1999), which is limited compared to that of quartz sand, which ranges from 79 GPa to 103 GPa (Daphalapurkar *et al.*, 2011). The unit weight of PDMS is 965 kg/m^3. The stress enforced on the tests could damage the polymer coatings and affect the behaviour of coated sand.

To predict the mechanical behaviour for coated sand, triaxial tests were carried out in saturated conditions to eliminate the effect of suction. The effect of stress level was considered. Critical state soil mechanics is used to predict the mechanical behaviour (Been *et al.*, 1991; Jefferies & Been, 2000), while the critical state is identified following Schofield & Wroth (1968) and Wood (1990). The critical state locus (CSL) in the q–p' plane is shown in equation (1).

$$q = M p' \tag{1}$$

Mean effective stress at critical state p'_{cs} is used to reflect the stress level applied to the sand grains.

In the e–lnp' plane, the CSL is represented through a linear function, as shown in equation (2).

$$e = \Gamma - \lambda \ln p' \tag{2}$$

For a given soil, equations (1) and (2) can provide a thorough description of the CSL.

Lourenço *et al.* (2018) showed that the polymer coatings smooth the surface of the natural sand, decreasing its roughness. Cavarretta *et al.* (2010) and Altuhafi *et al.* (2016) highlighted that roughness does not have a significant effect on sand behaviour, with the influence of particle shape dominating over roughness. In this note, it is hypothesised that, as the polymer coatings are damaged under high stresses, the mechanical behaviour converges to that of an uncoated, natural sand. To verify the hypothesis, the surface topology is imaged with white light interferometry (Fogale Nanotech, France).

The objectives of this paper are: (*a*) to investigate the effect of polymer coatings on soil behaviour (CSLs in q–p' and e–lnp' planes) and (*b*) to investigate the influence of the stress

Manuscript received 18 January 2018; revised manuscript accepted 18 October 2018. Published online ahead of print 27 November 2018.
Discussion on this paper closes on 1 February 2020, for further details see p. ii.
* Department of Civil Engineering, The University of Hong Kong, Hong Kong SAR, PR China.
† Department of Civil Engineering, The University of Hong Kong, Hong Kong SAR, PR China (Orcid:0000-0002-7534-8760).
‡ Department of Civil Engineering, The University of Hong Kong, Hong Kong SAR, PR China (Orcid:0000-0002-0250-5809).

level on the polymer coatings and consequent influence on the mechanical behaviour.

TESTING MATERIALS AND PROGRAMME

Sand and coating synthesis

Dichlorodimethylsilane (DMDCS), which has been used in the treatment of soils, was mixed with the wettable sand in a predetermined proportion to produce the PDMS-based coatings (with a water-repellent behaviour) (Ng & Lourenço, 2016). The sessile drop method was used to quantify the water repellency level by measuring the contact angle (CA) of water drops resting on a layer of particles (Leelamanie *et al.*, 2008; Saulick *et al.*, 2017). The level of water repellency is determined by the mass ratio of DMDCS. The CA increases with the rise of mass ratio of DMDCS, with the CA reaching its maximum and remaining stable. The relationship between the mass ratio of DMDCS and CAs for Fujian sand is shown in Fig. 1.

Figure 1 shows that the maximum CA is approximately 114° when the mass ratio of DMDCS is higher than 0·05%. Taking 0·05% as a threshold, three materials were selected for this paper: (*a*) wettable natural Fujian sand (Sinoma, China), which is a quartz sand with particle size between 1·18 and 2 mm; (*b*) 0·05% coated sand, representing the lower mass ratio threshold to induce extreme water repellency; (*c*) 3% coated sand, also with extreme water repellency, but to investigate the effect of the polymer coatings' thickness (Fig. 2).

Given the inability to measure directly the thickness of the polymer coating, the thickness was estimated by way of a technique proposed by Bardet *et al.* (2014) using equation (3).

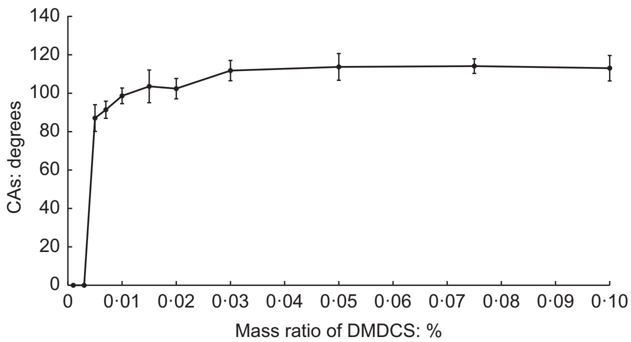

Fig. 1. Relationship between mass ratio of DMDCS and CAs for Fujian sand

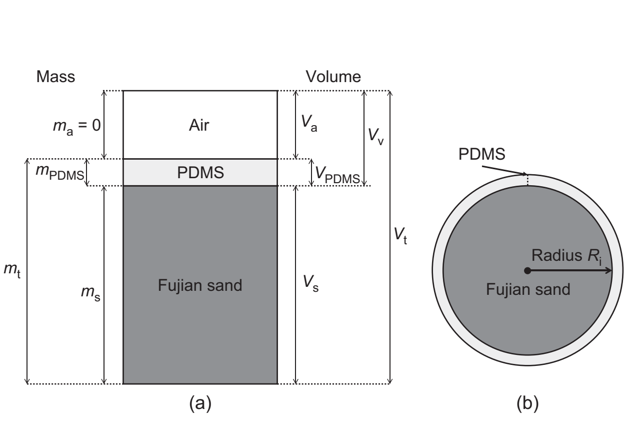

Fig. 2. Coated particles phase relations (modified from Bardet *et al.*, 2014): (a) air, PDMS and solid components; (b) idealised spherical coated particle

$$w' = \frac{p_{PDMS}}{p_s}\left[\sum_{i=1}^{N} p_i\left(1+\frac{t_i}{R_i}\right)^3 - 1\right] \tag{3}$$

where $w' = (m_{PDMS}/m_s)$; p_{PDMS} is the unit mass of PDMS; p_s is the unit mass of a particle; N_i is the number of particles with a radius R_i; p_i is the percentage by weight for a radius R_i; and t_i is the polymer coating's thickness. When the mass ratio of DMDCS is 0·05%, the thickness of the polymer coating varies between 163 and 277 nm, whereas for a DMDCS mass ratio of 3%, the thickness of the polymer coating is in the range 9·636–16·331 μm. The polymer coatings are very thin films compared to the sand size. The specific gravities (G_s) of

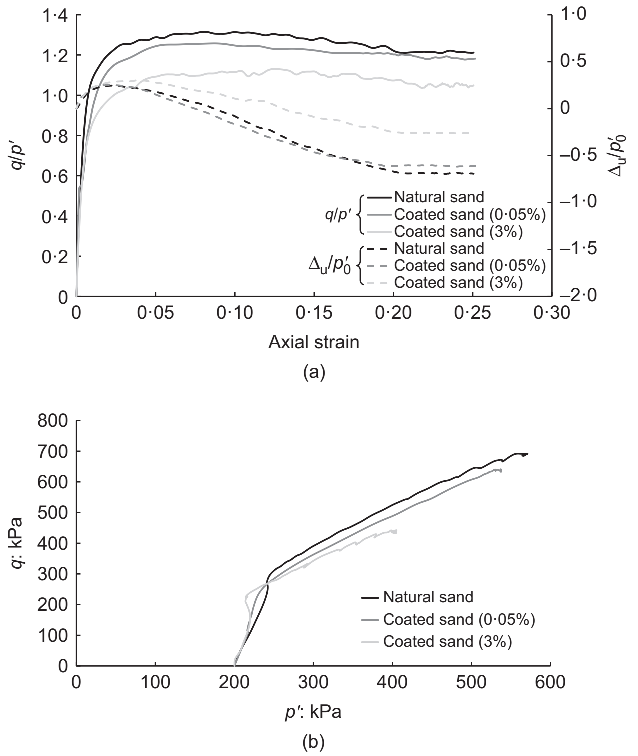

Fig. 3. Shearing behaviour (p'_0 = 200 kPa, $e \approx 0{\cdot}711$): (a) stress–strain relation; (b) stress path

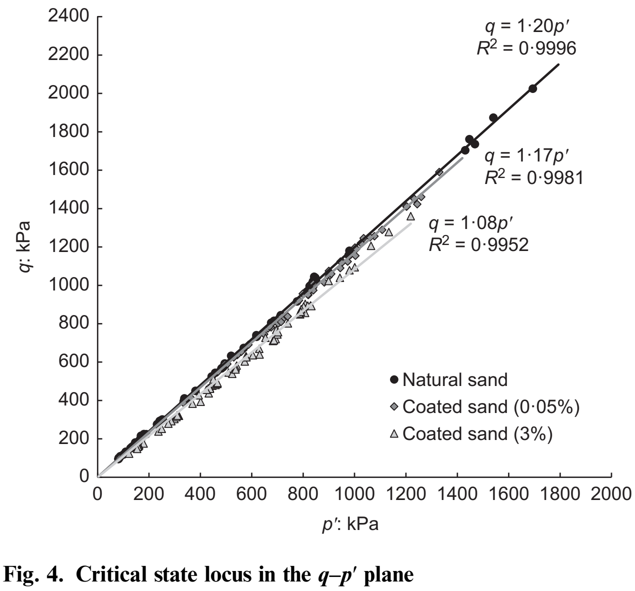

Fig. 4. Critical state locus in the *q*–*p′* plane

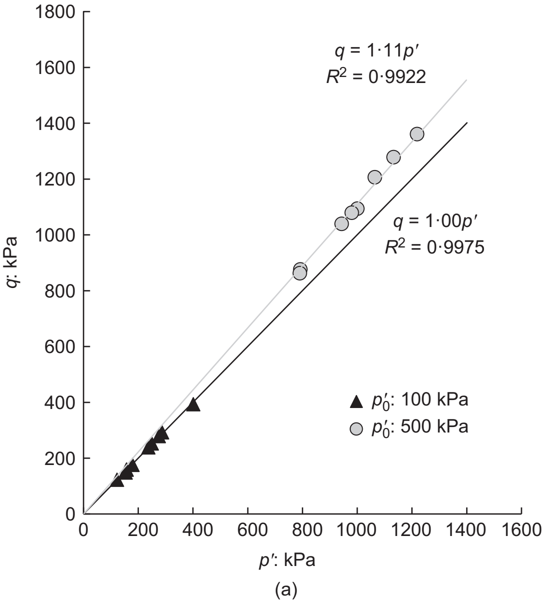

Fig. 5. The effect of stress level on the 3% coated sand: (a) CSLs fitted with linear functions when p'_0 is 100 and 500 kPa, respectively; (b) CSL fitted with a curved function

the three testing materials were experimental quantified, resulting in a $G_s = 2{\cdot}66$. Therefore, the impact of polymer coatings on G_s is negligible.

Triaxial testing

All specimens were prepared by the moist tamping method using the under-compaction technique (Ladd, 1974). Relatively high back-pressure (i.e. 600–800 kPa) was applied to the sample in case the water-repellent behaviour could influence the degree of saturation. The results show that water repellency did not affect the saturation stage. *B*-values were greater than 0·98 for each test. The post-consolidation void ratio was determined based on the method proposed by Yang & Wei (2012). Triaxial tests were conducted at various initial effective consolidation pressures p'_0 and various target initial void ratios.

Roughness measurement

The roughness of the natural and coated sands (3%) collected prior to and after the triaxial tests was quantified directly through white light interferometry. Given the nano-sized thickness of the polymer coatings, surface roughness was not measured for a DMDCS mass ratio of 0·05%. The dimensions of the field of view were 106·6 μm × 141·5 μm and the root-mean-square roughness (S_q) was selected to represent the surface roughness (Yang & Baudet, 2016). For both natural and coated sand (3%), roughness and *M*-values were measured with various p'_0 and similar void ratio to investigate the effect of stress levels on the polymer coatings.

RESULTS AND DISCUSSION

Shearing behaviour

Figure 3 shows the results for three typical undrained tests with different mass ratio of DMDCS; the p'_0 is 200 kPa and the post-consolidation void ratio is approximately 0·711. Fig. 3(a) shows that all three specimens tend towards the critical state in which the final stress ratios were fairly constant. For coated sand (0·05%), the stress ratio is slightly smaller than that of natural sand. For coated sand (3%), a significant reduction of stress ratio is observed. The excess pore pressure for the three materials shows a similar tendency and Fig. 3(b) shows that natural sand is more dilative than the coated sand.

Critical state locus in the q–p′ plane

The CSLs in the *q–p′* plane of the three materials acquired through both drained (CD) and undrained (CU) tests are shown in Fig. 4. For natural sand, all data points are fitted by a linear function with 0 intercept. The CSL is independent of drainage conditions and p'_{cs}. The *M*-value for natural sand is 1·20.

For coated sand (0·05%), the effect of the polymer coatings on CSL is not significant, with all data points fitted by a linear function with 0 intercept, and *M*-values for the coated sand (0·05%) of 1·17, which is slightly smaller than that of natural sand. This agrees with the results from the stress–strain behaviour.

For coated sand (3%), all data points are fitted in a linear function with 0 intercept. *M*-value for the coated sand

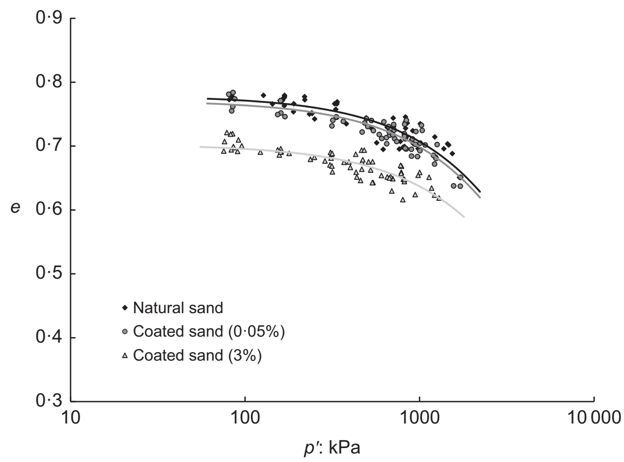

Fig. 6. Critical state locus in the *e*–ln*p′* plane

(3%) is 1·08, which indicates that the *M*-values of coated sand decrease with the rise of mass ratio of DMDCS. Although the R^2 is 0·9952, the effect of stress level on the polymer coatings can be discerned. For instance, as shown in Fig. 5(a), the *M*-value of tests conducted when $p_0' = 100$ kPa is 1·00, while the *M*-value of tests conducted when $p_0' = 500$ kPa is 1·11. The effect of stress level on the polymer coatings and consequent *M*-values is significant.

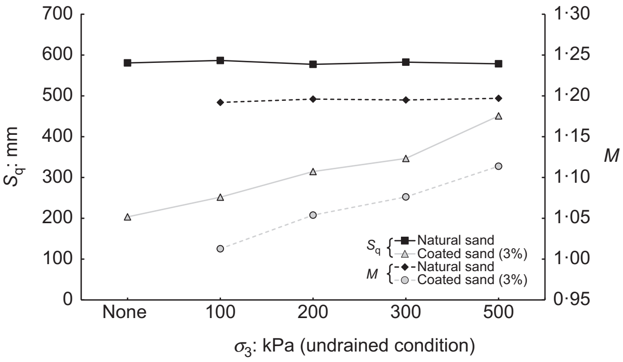

Fig. 7. Quantification of roughness and variation of *M*-values

Fu *et al*. (2017) proposed that a curved line could be used to fit the CSL for sand–rubber mixtures. Given the similarity between rubber and PDMS, an alternative interpretation of the results is shown in Fig. 5(b), with a curved line drawn to show the CSL for the coated sand (3%). The curved line shows that the *M*-values of coated sand (3%) are stress level dependent. When the stress level is sufficiently high, the *M*-values would be similar to those of natural sand, which suggests that the polymer coatings are severely damaged, and the effect of polymer coatings diminishes.

Critical state locus in the e–ln*p*′ *plane*

Figure 6 illustrates the CSLs in the *e*–ln*p*′ plane. As granular materials, the CSLs in the *e*–ln*p*′ plane are initially curved. The results show that when the mass ratio is 0·05%, the effect of polymer coatings on the CSL in the *e*–ln*p*′ plane is not significant. In contrast, when the mass ratio is 3%, the effect of the polymer coatings on the CSL is considerable, with the intercept of the CSL reducing remarkably compared to that of natural sand. In addition, the CSLs tend towards that of natural sand with the rise of stress level. This effect is less significant, however, which could be attributed to the fact that most tests conducted reached a critical state on the flatter part of the CSLs, with the stress level not high enough to totally damage the polymer coatings.

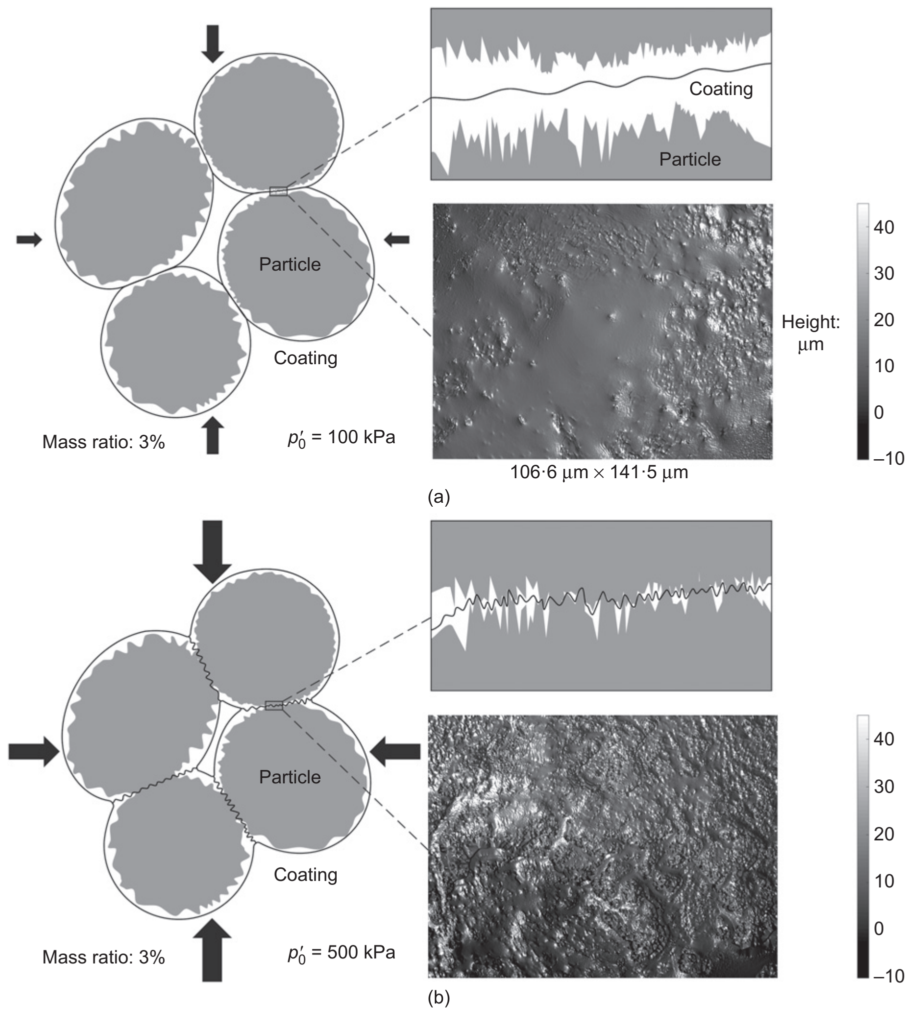

Fig. 8. Schematic drawing illustrating the effect of the stress level on the 3% coated sand (not drawn to scale): (a) p_0' is 100 kPa; (b) p_0' is 500 kPa (left-hand side: idealised coated sand particles; right-hand side: amplified contacts and surface topology of real coated sand (3%) particles)

Effect of stress level on polymer coatings

Figure 7 shows the effect of stress level on polymer coatings. In an undrained condition, for natural sand, both S_q and M-values remain constant regardless of p'_0 (i.e. p'_{cs}). For coated sand (3%), the effect of stress level on roughness and M-values is significant. For instance, when p'_0 is 100 kPa, the M-value and S_q are only 1·01 and 203·54 nm, respectively, which are small compared to those of natural sand. As shown in Fig. 8(a), the damage to the polymer coatings is negligible, as exemplified by a smooth surface topology, and the polymer coatings are intact. When p'_0 is 500 kPa, the M-value and S_q are 1·11 and 450·92 nm, respectively. As shown in Fig. 8(b), the polymer coatings are considerably damaged, both S_q and M-values converge towards those of natural sand (1·20 and 580·76 nm), with the surface topology becoming rougher. This result verifies the hypothesis that the polymer coatings, by smoothing the particles, cause a decrease in the M-values, with this effect diminishing as the polymer coatings are scratched under stress.

CONCLUSION

This paper presents an experimental investigation on coated sands. The results are summarised as follows.

(*a*) For a mass ratio of 0·05% DMDCS, the shearing behaviour of coated sand (0·05%), CSLs in both the q–p' and the e–lnp' plane are similar to those of natural sand. The fact that 0·05% mass ratio of DMDCS is sufficiently high to make the sand extremely water repellent suggests that coated sand (0·05%) is appropriate for use in geotechnical applications.

(*b*) For a mass ratio of 3% DMDCS, the reduction of shear strength is evident, and the CSLs of coated sand (3%) in both q–p' and e–lnp' planes show a significant difference compared to those of natural sand, which is due to the presence of the thicker polymer coatings. Furthermore, the roughness measurements reflect the damage to the polymer coatings. The mechanical behaviour of coated sand (3%) converges to that of natural sand with a rise of stress level, which suggests that the effect of polymer coatings diminishes gradually. While coated sand (3%) does not translate into benefits in terms of wetting behaviour, the stress dependency opens the possibility of using them to manipulate soil behaviour for other, targeted applications.

ACKNOWLEDGEMENT

Financial support provided by the General Research Fund, Research Grants Council, Hong Kong (17200114, 17221016, T22-603/15-N) is acknowledged.

NOTATION

- e void ratio
- G_s specific gravity
- M effective stress ratio at the critical state
- m_a mass of air
- m_{PDMS} mass of PDMS
- m_s mass of dry sand
- m_t total mass
- N_i number of particles with a radius R_i
- p' mean effective stress
- p'_{cs} mean effective stress at critical state
- p_i percentage by weight for a radius R_i
- ρ_{PDMS} unit mass of polydimethylsiloxane
- ρ_s unit mass of particle
- p'_0 initial effective consolidation pressure
- q deviatoric stress
- R_i radius of particles
- S_q root-mean-square roughness
- t_i thickness of polymer coatings
- V_a volume of voids occupied by air
- V_{PDMS} volume of PDMS
- V_s volume of particles
- V_t total volume
- w' estimated thickness of polymer layer
- Γ void ratio intercept
- λ slope of the CSL in the e–lnp' plane

REFERENCES

Altuhafi, F. N., Coop, M. R. & Georgiannou, V. N. (2016). Effect of particle shape on the mechanical behavior of natural sands. *J. Geotech. Geoenviron. Engng* **142**, No. 12, 04016071.

Armani, D., Liu, C. & Aluru, N. (1999). Re-configurable fluid circuits by PDMS elastomer micromachining. In *IEEE international MEMS 99 conference. Twelfth IEEE international conference on micro electro mechanical systems*. pp. 222–227. Piscataway, NJ, USA: Institute of Electrical and Electronics Engineers.

Bardet, J. P., Benazza, C., Bruchon, J. F. & Mishra, M. (2009). Mechanical and hydraulic properties of wax-coated sands for sport surfaces. In *Powders and grains 2009: Proceedings of the 6th international conference on micromechanics of granular media* (eds M. Nakagawa and S. Ludwig), AIP Conference Proceedings, vol. 1145, pp. 792–795. College Park, MD, USA: American Institute of Physics.

Bardet, J. P., Jesmani, M. & Jabbari, N. (2011). Effects of compaction on shear strength of wax-coated sandy soils. *Electron. J. Geotech. Engng* **16**, Bundle D, 451–461.

Bardet, J. P., Jesmani, M. & Jabbari, N. (2014). Permeability and compressibility of wax-coated sands. *Géotechnique* **64**, No. 5, 341–350, https://doi.org/10.1680/geot.13.P.118.

Been, K., Jefferies, M. G. & Hachey, J. (1991). The critical state of sands. *Géotechnique* **41**, No. 3, 365–381, https://doi.org/10.1680/geot.1991.41.3.365.

Byun, Y. H., Tran, M. K., Yun, T. S. & Lee, J. S. (2011). Strength and stiffness characteristics of unsaturated hydrophobic granular media. *Geotech. Testing J.* **35**, No. 1, 193–200.

Cavarretta, I., Coop, M. & O'Sullivan, C. (2010). The influence of particle characteristics on the behaviour of coarse grained soils. *Géotechnique* **60**, No. 6, 413–423, https://doi.org/10.1680/geot.2010.60.6.413.

Daphalapurkar, N. P., Wang, F., Fu, B., Lu, H. & Komanduri, R. (2011). Determination of mechanical properties of sand grains by nanoindentation. *Expl Mech.* **51**, No. 5, 719–728.

Doerr, S. H., Shakesby, R. A. & Walsh, R. P. D. (2000). Soil water repellency: its causes, characteristics and hydro-geomorphological significance. *Earth Sci. Rev.* **51**, No. 1–4, 33–65.

Fu, R., Coop, M. R. & Li, X. Q. (2017). Influence of particle type on the mechanics of sand–rubber mixtures. *J. Geotech. Geoenviron. Engng* **143**, No. 9, 04017059.

Jefferies, M. & Been, K. (2000). Implications for critical state theory from isotropic compression of sand. *Géotechnique* **50**, No. 4, 419–429, https://doi.org/10.1680/geot.2000.50.4.419.

Ladd, R. S. (1974). Specimen preparation and liquefaction of sands. *J. Geotech. Engng Div.* **100**, No. 10, 1180–1184.

Lechman, J., Lu, N. & Wu, D. (2006). Hysteresis of matric suction and capillary stress in monodisperse disk-shaped particles. *J. Engng Mech.* **132**, No. 5, 565–577.

Lee, C., Yang, H. J., Yun, T. S., Choi, Y. & Yang, S. (2015). Water-entry pressure and friction angle in an artificially synthesized water-repellent silty soil. *Vadose Zone J.* **14**, No. 4, https://doi.org/10.2136/vzj2014.08.0106.

Leelamanie, D. A. L., Karube, J. & Yoshida, A. (2008). Characterizing water repellency indices: contact angle and water drop penetration time of hydrophobized sand. *Soil Sci. Pl. Nutr.* **54**, No. 2, 179–187.

Lötters, J. C., Olthuis, W., Veltink, P. H. & Bergveld, P. (1997). The mechanical properties of the rubber elastic polymer polydimethylsiloxane for sensor applications. *J. Micromech. Microengng* **7**, No. 3, 145.

Lourenço, S. D. N., Saulick, Y., Zheng, S., Kang, H., Liu, D., Lin, H. & Yao, T. (2018). Soil wettability in ground engineering: fundamentals, methods, and applications. *Acta Geotechnica* **13**, No. 1, 1–14.

Ng, S. H. Y. & Lourenço, S. D. N. (2016). Conditions to induce water repellency in soils with dimethyldichlorosilane. *Géotechnique* **66**, No. 5, 441–444, https://doi.org/10.1680/jgeot.15.T.025.

Saulick, Y., Lourenço, S. D. N. & Baudet, B. A. (2017). A semi-automated technique for repeatable and reproducible contact angle measurements in granular materials using the Sessile drop method. *Soil Sci. Soc. Am. J.* **81**, No. 2, 241–249.

Schofield, A. & Wroth, P. (1968). *Critical state soil mechanics.* London, UK: McGraw-Hill.

Wood, D. M. (1990). *Soil behaviour and critical state soil mechanics.* Cambridge, UK: Cambridge University Press.

Yang, H. & Baudet, B. A. (2016). Characterisation of the roughness of sand particles. *Procedia Engng* **158**, 98–103.

Yang, J. & Wei, L. M. (2012). Collapse of loose sand with the addition of fines: the role of particle shape. *Géotechnique* **62**, No. 12, 1111–1125, https://doi.org/10.1680/geot.11.P.062.

Zheng, S., Lourenço, S. D., Cleall, P. J., Chui, T. F. M., Ng, A. K. & Millis, S. W. (2017). Hydrologic behavior of model slopes with synthetic water repellent soils. *J. Hydrol.* **554**, 582–599.